Second Harmonic Generation and Magnetic-Dipole–Electric-Dipole Interference in Antiferromagnetic Cr_2O_3

M. Fiebig and D. Fröhlich
Institut für Physik, Universität Dortmund, 44221 Dortmund, Germany

B. B. Krichevtsov and R. V. Pisarev
Ioffe Physical Technical Institute of the Russian Academy of Sciences, St. Petersburg 194021, Russia
(Received 7 June 1994)

The second harmonic spectrum of Cr_2O_3 is studied in the 1.7–2.9 eV spectral range as a function of temperature. Below the Néel temperature $T_N = 307.5$ K a nonlinear electric susceptibility $\chi^e_{ijk}(c)$ appears, which changes sign under the time-reversal operation. The interference of this susceptibility with the time-invariant magnetic susceptibility $\chi^m_{ijk}(i)$ leads to a pronounced polarization dependence for circularly polarized light propagating along the optical axis. This gives a novel tool to study antiferromagnetic domains with opposite orientation of the order parameter.

PACS numbers: 75.60.Ch, 42.65.Ky, 75.50.Ee

Nonlinear optical susceptibilities of *magnetic* origin, related to a magnetic field of the light wave or to magnetic ordering in a crystal, possess quite different transformation properties under space and time symmetry operations than nonlinear susceptibilities of *electric* origin. These differences stem from different behavior of electric- and magnetic-dipole transitions under these symmetry operations and the specific features of optical nonlinearities of magnetic materials. These features have been discussed theoretically for quite a long time in the case of bulk crystals and magnetized surfaces [1–10], but the experimental data so far are restricted to measurements on surfaces and thin films at a single frequency. Optical second harmonic generation (SHG) was observed in thin films of magnetic garnets in reflection and transmission experiments [11–13]. It was demonstrated in several metallic magnetic materials that the intensity of the second harmonic (SH) is sensitive to the surface magnetization [14–16].

Depending on the crystallographic and the magnetic structure of the material under study, one expects different contributions to nonlinear susceptibilities from electric- and magnetic-dipole transitions above and below the magnetic transition temperature. The contribution of *magnetic-dipole* transitions was usually neglected in comparison with the *electric-dipole* transitions. In case of *d-d* transitions in magnetics, however, these two contributions may be comparable since in a first approximation electric-dipole transitions are parity forbidden, but magnetic-dipole transitions may be allowed. A separation of these contributions is difficult in experiments which are carried out at only one or several discrete photon energies. A deeper insight into the microscopic nature of optical nonlinearities can be reached in *spectroscopic* studies in an extended spectral range which covers optical transitions between different electronic levels.

In this Letter we report the first experimental observation of the spectral and temperature dependence of the nonlinear optical susceptibilities in a magnetically ordered substance. Measurements were performed on antiferromagnetic Cr_2O_3. Our conclusions, however, are of general nature and therefore valid for other magnetics. Experimental data allow us to distinguish quite clearly between the contributions of different transitions to both *time-invariant* (i-type) and *time-noninvariant* (c-type) nonlinear susceptibilities [17]. The SH spectra differ significantly from linear absorption spectra. Since the interference between contributions of i and c types may give rise to SHG which depends *linearly* on the relevant order parameter and allows the distinction between magnetic states related to each other by the time-reversal symmetry operation $\underline{1}$.

Above the Néel temperature T_N Cr_2O_3 crystallizes in the centrosymmetric point group $\bar{3}m$ [17–19]. Axial i tensors of odd rank and polar i tensors of even rank are allowed in this point group [2,17]. Thus above T_N nonlinear electric-dipole effects due to χ^e_{ijk} (polar i tensor) are forbidden, but magnetic-dipole effects due to χ^m_{ijk} (axial i tensor) are allowed. One, therefore, may expect SHG from a magnetic-dipole contribution due to $\chi^m_{ijk}(i)$ above T_N. Below T_N, however, four spins in the unit cell order along the optical axis in a noncentrosymmetric antiferromagnetic structure [18–20]. The antiferromagnetic vector $\mathbf{l}_2$ is also oriented along the optical axis. This leads to two types of domains transformed into each other by the time-reversal operation. Both space- and time-reversal symmetry operations are simultaneously broken, but the combined space-time-reversal operation $\bar{\underline{1}}$ remains a symmetry element. The magnetic point group of Cr_2O_3 is $\bar{3}\underline{m}$. In this point group new phenomena described by polar c tensors of odd rank and axial c tensors of even rank are allowed. For example, the existence of a polar c tensor of second rank leads to the static magnetoelectric effect in Cr_2O_3 [19]. In addition to magnetic-dipole effects due to χ^m_{ijk} (axial i tensor) electric-dipole effects due to χ^e_{ijk} (polar c tensor) are allowed below T_N [2,17].

0031-9007/94/73(15)/2127(4)$06.00

In the following, we will derive the equations for SHG in the point group $\bar{3}m$ for magnetic- and electric-dipole contributions. We restrict the analysis to light propagating along the optical axis (z axis). Thus only one independent component $\chi_m(i) \equiv \chi^m_{yyy}(i) = -\chi^m_{yxx}(i) = -\chi^m_{xyx}(i) = -\chi^m_{xxy}(i)$ of the nonlinear susceptibility [17] contributes to the nonlinear magnetization

$$\mathbf{M}_{\mathrm{NL}} = \epsilon_0 \frac{c}{n} \begin{pmatrix} -2\chi_m(i) E_x E_y \\ -\chi_m(i)(E_x^2 - E_y^2) \\ 0 \end{pmatrix}, \quad (1)$$

where c/n is the speed of light in the crystal at the laser frequency and E_x and E_y are the electric field components along the x and y axis, respectively. In the wave equation for the electric field the magnetic-dipole contribution leads to a source term $\mu_0 \nabla \times \partial \mathbf{M}_{\mathrm{NL}}/\partial t$ for SHG [1,2]. Since this source term is allowed above and below T_N, it should not induce any anomalous change of the SHG when going from the paramagnetic to the antiferromagnetic state. Below T_N, however, there is an additional source term which is due to the breaking of space-inversion symmetry. Since this breaking is due to magnetic ordering, the relevant tensor $\chi^e_{ijk}(c)$ is of c type [17] and depends linearly on the order parameter. It leads to a nonlinear polarization $\mathbf{P}_{\mathrm{NL}}$. For light propagating along the z axis $\mathbf{P}_{\mathrm{NL}}$ is given by one independent component $\chi_e(c) \equiv \chi^e_{yyy}(c) = -\chi^e_{yxx}(c) = -\chi^e_{xyx}(c) = -\chi^e_{xxy}(c)$ [17] of the nonlinear susceptibility

$$\mathbf{P}_{\mathrm{NL}} = \epsilon_0 \begin{pmatrix} -2\chi_e(c) E_x E_y \\ -\chi_e(c)(E_x^2 - E_y^2) \\ 0 \end{pmatrix}. \quad (2)$$

In the wave equation the electric-dipole contribution leads to the source term $\mu_0(\partial^2 \mathbf{P}_{\mathrm{NL}}/\partial t^2)$ for SHG. With plane waves for the incoming laser fields one can derive the total source term

$$\mathbf{S} = \mu_0 \left(\nabla \times \frac{\partial \mathbf{M}_{\mathrm{NL}}}{\partial t} + \frac{\partial^2 \mathbf{P}_{\mathrm{NL}}}{\partial t^2} \right) = 4\frac{\omega^2}{c^2} \begin{pmatrix} \chi_m(i)(E_x^2 - E_y^2) + 2\chi_e(c) E_x E_y \\ -2\chi_m(i) E_x E_y + \chi_e(c)(E_x^2 - E_y^2) \\ 0 \end{pmatrix}, \quad (3)$$

where $\hbar\omega$ is the energy of the incoming light beam. The polarization selection rules become simpler if one rewrites the total source term in a circular basis with $\mathbf{E} = E_+ \mathbf{e}_+ + E_- \mathbf{e}_- + E_z \mathbf{e}_z$, where $\mathbf{e}_+ = -(1/\sqrt{2})(\mathbf{e}_x + i\mathbf{e}_y)$ and $\mathbf{e}_- = (1/\sqrt{2})(\mathbf{e}_x - i\mathbf{e}_y)$. One gets

$$\mathbf{S} = \begin{pmatrix} S_+ \\ S_- \\ S_z \end{pmatrix} = 4\sqrt{2}\frac{\omega^2}{c^2} \begin{pmatrix} [-\chi_m(i) + i\chi_e(c)] E_-^2 \\ [+\chi_m(i) + i\chi_e(c)] E_+^2 \\ 0 \end{pmatrix}. \quad (4)$$

Incoming left circularly polarized light leads to right circularly polarized light at the second harmonic and vice versa. In case of resonance SHG both susceptibilities are complex tensors ($\chi = \chi' + i\chi''$) which depend on the total photon energy $2\hbar\omega$ in a different way. From the solution of the wave equation with the source term $\mathbf{S}$ [Eq. (4)] one gets for a highly absorbing medium $I \propto |\mathbf{S}|^2$ [3], i.e.,

$$I \propto [|\chi_m(i)|^2 + |\chi_e(c)|^2][|E_+|^4 + |E_-|^4] - 2[\chi'_m(i)\chi''_e(c) - \chi''_m(i)\chi'_e(c)][|E_+|^4 - |E_-|^4]. \quad (5)$$

The first term is quadratic in $\chi_m(i)$ and $\chi_e(c)$ and is always positive. The second term is linear in $\chi_m(i)$ and $\chi_e(c)$ and may vary from zero for linearly polarized light to its positive or negative maximum value for circularly polarized light. It is thus referred to as an interference term. If we restrict ourselves to the use of circularly polarized light of intensity I_σ we can rewrite Eq. (5) as function of the circular polarization ($\sigma = \pm 1$) and of the direction ($l = \pm 1$) of the antiferromagnetic vector [18,19]

$$I(l, \sigma) \propto I_\sigma^2 [|\chi_m(i)|^2 + |\chi_e(c)|^2 - \Delta(l)\sigma], \quad (6)$$

where $\Delta(l) = 2[\chi'_m(i)\chi''_e(c) - \chi''_m(i)\chi'_e(c)]$. The magnetic and the electric contribution may interfere in a constructive or destructive way. The sign of the interference contribution $\Delta(l)\sigma$ can be changed either by reversing the circular polarization σ or by the time-reversal operation, which is equivalent to a reversal of the antiferromagnetic vector $\mathbf{l}_2$. The two types of domains which are described by a different orientation of $\mathbf{l}_2$ should therefore reveal the same SH spectra but with a reversed dependence on the circular polarization.

The experimental setup is shown schematically in Fig. 1. An optical parametric oscillator (OPO) and a tunable dye laser are pumped by a frequency-tripled Nd-doped yttrium-aluminium-garnet (YAG) laser. The tunable dye laser is used for seeding the OPO which results in its narrow bandwidth ($\Delta E \approx 10$ μeV). Synchronized tuning of the OPO and the dye laser is controlled by a computer. Optical filters and a monochromator are used for suppression of scattered laser light. Quarter- and half-wave plates are used to set the helicity of the incoming laser beam and to analyze the light at the second harmonic. X-ray-oriented bulk samples with thicknesses between 70 μm and 1.2 mm were cut perpendicular to the optical axis from boules of Cr_2O_3 grown by the Verneuil

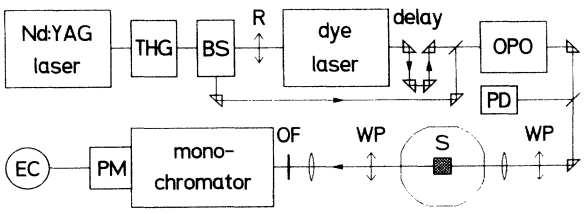

FIG. 1. Schematic diagram of the experimental setup. BS, beam splitter; EC, electronics and computer; OF, optical filter; OPO, optical parametric oscillator; PD, photodiode; PM, photomultiplier; R, rotator of polarization; S, sample; THG, third harmonic generator; WP, quarter- or half-wave plate.

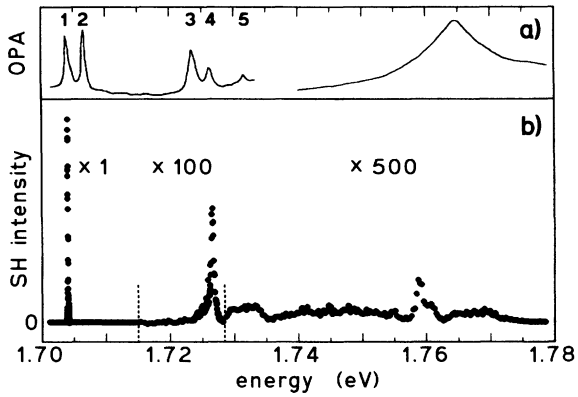

FIG. 2. (a) One-photon absorption (OPA) spectrum of Cr_2O_3 at $T = 77$ K; left part from [22], right part from [21]. (b) SH spectrum at $T = 10$ K for wave vector parallel to the z axis. Note change of scale at 1.715 and 1.728 eV.

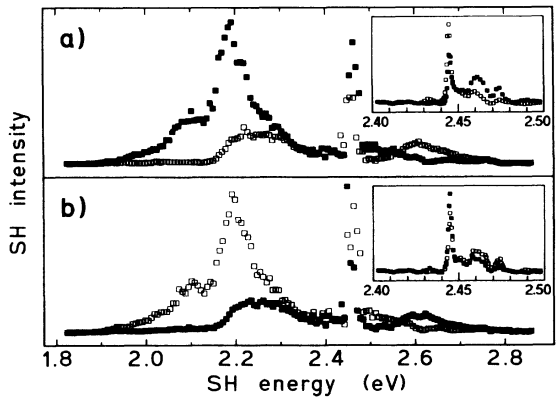

FIG. 3. SH spectrum of Cr_2O_3 for wave vector parallel to the z axis. Full and open squares refer to right and left circularly polarized light of the incoming laser beam, respectively. (a) and (b) correspond to two domains with opposite orientation of the antiferromagnetic vector. Inset shows $^2T_2$ transitions.

method. The SH spectra were measured in a temperature range 10–325 K by use of a closed-cycle refrigerator. Light was incident along the optical axis of the crystals.

We will now present experimental results for two spectral regions which differ drastically in their polarization behavior. Figure 2 shows the low temperature SH spectrum in the region of the spin-forbidden $^4A_2 \rightarrow {}^2E$ transition. The linear absorption spectrum of this transition was studied previously in detail [21–23]. The strongest SH line at 1.704 eV has a spectral width of only 40 μeV. It corresponds to the σ-polarized line 1 [22]. Weaker peaks correspond to the σ-polarized lines 4 and 5. These lines 1, 4, and 5 obey the selection rules of an electric-dipole transition. No SHG was detected for the π-polarized lines 2 and 3. There was no dependence on the circular polarization of the incoming light. This means that only the $|\chi_e(c)|^2$ contribution to the SH intensity is effective in this part of the spectrum [Eq. (6)]. Since this contribution is quadratic with respect to the order parameter, it decreases rapidly with increasing temperature and the SH signal disappears at about 250 K.

Figure 3 shows the SH spectrum at $T \approx 10$ K for incoming light with two circular polarizations in the range 1.8–2.9 eV which includes several spin-forbidden and spin-allowed transitions ($^4A_2 \rightarrow {}^2T_1$, $^4T_2$, $^2T_2$, and $^4T_1$). As expected from Eq. (4) the light at the second harmonic is circularly polarized but with opposite helicity with respect to the incoming light. Contrary to the SH spectra of the $^4A_2 \rightarrow {}^2E$ transition there is a pronounced polarization dependence. Measurements of the SH intensity as a function of temperature (Fig. 4) revealed a decrease of the sum of both intensities $I = I(+) + I(-)$ when the temperature was increased. Moreover, at $T_N = 307.5 \pm 1.0$ K the polarization dependence vanishes although a SH signal was detected at even higher temperature. Above T_N the SH signal in the region of the $^4A_2 \rightarrow {}^4T_2$ transition obeys the selection rules of a magnetic-dipole transition.

The rather spectacular polarization dependence is fully explained by Eq. (6). Above T_N only $|\chi_m(i)|^2$ contributes to the SH signal. Since Δ vanishes [$\chi_e(c) = 0$] no polarization dependence is expected. Below T_N, however, $\chi_e(c)$ also contributes to the SHG. In the spectral region of resonances $\chi_m(i)$ and $\chi_e(c)$ are both complex. In the region of overlapping resonances one thus expects a dependence on the circular polarization and on the orientation of the order parameter due to the interference contribution $\Delta(l)\sigma$. Since $\chi_e(c)$ depends linearly on the order parameter, $\Delta(l)$ also depends linearly on it, which leads to a change of sign of $\Delta(l)$ if the laser spot is moved to another domain. By scanning the laser spot across the sample we indeed observed the expected interchange of the circular polarization dependence due to domain walls (Fig. 3). By reversing the sample we could even show that it has single domains along the z axis.

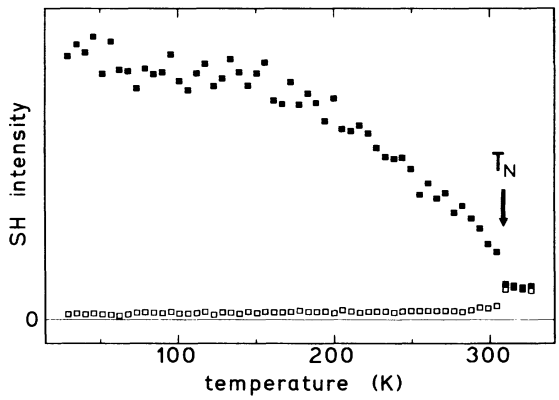

FIG. 4. Temperature dependence of the SH intensity of Cr_2O_3 at 2.00 eV in one domain. The Néel temperature $T_N = 307.5$ K is marked by an arrow. Full and open squares refer to right and left circularly polarized light of the incoming laser beam, respectively.

In order to model the spectral and temperature dependence of the interference contribution we used two different Lorentzians for $\chi_m(i)$ and $\chi_e(c)$. We took a linear temperature dependence of $\chi_e(c)$ on the order parameter [24]. Even with this simple model the basic features of our data are qualitatively reproduced.

In conclusion, we have studied the SH spectrum of Cr_2O_3 in a wide spectral range which includes d-d transitions to several spin-allowed and spin-forbidden bands. The SH spectrum differs significantly from the linear absorption spectrum [21,22], though several narrow lines were found in both spectra. We have shown that the SH spectrum arises due to different microscopic mechanisms such as magnetic- and electric-dipole transitions. Different mechanisms lead to different selection rules and a temperature dependence of the SH spectrum. We have shown that breaking of the time-reversal symmetry in the magnetically ordered state leads to a specific nonlinear electric susceptibility $\chi^e_{ijk}(c)$, which changes sign under the time-reversal operation $\underline{1}$. We have also observed that interference of this susceptibility with the time-invariant susceptibility $\chi^m_{ijk}(i)$ of magnetic-dipole character leads to a different output of the SH signal for right and left circularly polarized light propagating along the optical axis. Linear polarized light propagating along the optical axis should therefore exhibit nonlinear rotation and ellipticity. These effects as well as the observed effects change sign when going from one antiferromagnetic domain to another. The observed effects thus provide a rather unique tool to investigate antiferromagnetic domains and dynamical properties of domain walls with high spatial resolution. Our method is certainly not limited to Cr_2O_3, it should also be applicable to other magnetic materials which might show interference effects due to the existence of the appropriate tensor components of i and c type [2,17].

The financial support by the Deutsche Forschungsgemeinschaft and the Graduiertenkolleg "Festkörperspektroskopie" is greatly appreciated. The work of B. B. K. and R. V. P. was supported by the Russian Basic Research Foundation.

[1] P. S. Pershan, Phys. Rev. **130**, 919 (1963).
[2] E. B. Graham and R. E. Raab, Philos. Mag. **B66**, 269 (1992).
[3] Y. R. Shen, *The Principles of Nonlinear Optics* (Wiley, New York, 1984).
[4] S. Kielich and R. Zawodny, Opt. Acta **20**, 867 (1973).
[5] N. N. Akhmediev, S. B. Borisov, A. K. Zvezdin, I. L. Lyubchanskii, and Yu. V. Melikhov, Fiz. Tverd. Tela **27**, 1075 (1985) [Sov. Phys. Solid State **27**, 650 (1985)].
[6] S. B. Borisov, N. N. Dadoenkova, I. L. Lyubchanskii, and V. L. Sobolev, Fiz. Tverd. Tela **32**, 3668 (1990) [Sov. Phys. Solid State **32**, 2127 (1990)].
[7] S. S. Girgel and T. V. Demidova, Opt. Spektrosk. **62**, 101 (1987) [Opt. Spectrosc. (USSR) **62**, 63 (1987)].
[8] Ru-Pin Pan, H. D. Wei, and Y. R. Shen, Phys. Rev. B **39**, 1229 (1989).
[9] W. Hübner and K. H. Bennemann, Phys. Rev. B **40**, 5973 (1989).
[10] U. Pustogowa, W. Hübner, and K. H. Bennemann, Phys. Rev. B **48**, 8607 (1993); **49**, 10031 (1994).
[11] O. A. Aktsipetrov, O. V. Braginskii, and D. A. Esikov, Kvant. Elektron. (Moscow) **17**, 320 (1990) [Sov. J. Quantum Electron. **20**, 259 (1990)].
[12] R. V. Pisarev, B. B. Krichevtsov, V. N. Gridnev, V. P. Klin, D. Fröhlich, and Ch. Pahlke-Lerch, J. Phys. C **5**, 8621 (1993).
[13] G. Petrocelli, S. Martelucci, and M. Richetta, Appl. Phys. Lett. **63**, 3402 (1993).
[14] G. Spierings, V. Koutsos, H. A. Wierenga, M. W. J. Prins, D. Abraham, and Th. Rasing, Surf. Sci. **287/288**, 747 (1993); J. Magn. Magn. Mater. **121**, 109 (1993).
[15] J. Reif, C. Rau, and E. Matthias, Phys. Rev. Lett. **71**, 1931 (1993).
[16] J. Reif, J. C. Zink, C.-M. Schneider, and J. Kirschner, Phys. Rev. Lett. **67**, 2878 (1991).
[17] R. R. Birss, *Symmetry and Magnetism* (North-Holland, Amsterdam, 1964).
[18] I. E. Dzyaloshinskii, Zh. Eksp. Teor. Fiz. **32**, 1547 (1957) [Sov. Phys. JETP **5**, 1259 (1957)].
[19] I. E. Dzyaloshinskii, Zh. Eksp. Teor. Fiz. **37**, 881 (1959) [Sov. Phys. JETP **10**, 628 (1960)].
[20] L. M. Corliss, J. M. Hastings, R. Nathans, and G. Shirane, J. Appl. Phys. **36**, 1099 (1965).
[21] D. S. McClure, J. Chem. Phys. **38**, 2289 (1963).
[22] J. W. Allen, R. M. Macfarlane, and R. L. White, Phys. Rev. **173**, 523 (1969), and references therein.
[23] Y. Tanabe and K. Aoyagi, in *Excitons*, edited by V. M. Agranovich and A. A. Maradudin (North-Holland, Amsterdam, 1982), p. 603ff, and references therein.
[24] E. G. Samuelson, M. I. Hutchings, and G. Shirane, Physica (Utrecht) **48**, 13 (1970).

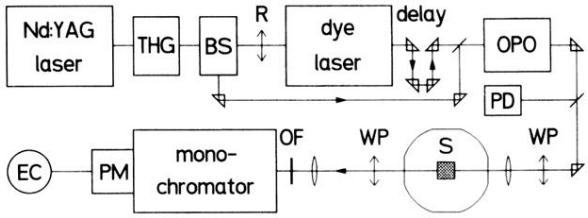

FIG. 1. Schematic diagram of the experimental setup. BS, beam splitter; EC, electronics and computer; OF, optical filter; OPO, optical parametric oscillator; PD, photodiode; PM, photomultiplier; R, rotator of polarization; S, sample; THG, third harmonic generator; WP, quarter- or half-wave plate.